Unconventional localization transition in high dimensions

S. V. Syzranov, V. Gurarie, and L. Radzihovsky
Physics Department, University of Colorado, Boulder, Colorado 80309, USA
(Received 2 December 2014; published 28 January 2015)

We study noninteracting systems with a power-law quasiparticle dispersion $\xi_{\mathbf{k}} \propto k^{\alpha}$ and a random short-range-correlated potential. We show that, unlike the case of lower dimensions, for $d > 2\alpha$, there exists a critical disorder strength (set by the bandwidth), at which the system exhibits a disorder-driven quantum phase transition at the bottom of the band that lies in a universality class distinct from the Anderson transition. In contrast to the conventional wisdom, it manifests itself in, e.g., the disorder-averaged density of states. For systems in symmetry classes that permit localization, the striking signature of this transition is a nonanalytic behavior of the mobility edge, which is pinned to the bottom of the band for subcritical disorder and grows for disorder exceeding a critical strength. Focusing on the density of states, we calculate the critical behavior (exponents and scaling functions) at this novel transition, using a renormalization group, controlled by an $\varepsilon = d - 2\alpha$ expansion. We also apply our analysis to Dirac materials, e.g., Weyl semimetals, where this transition takes place in physically interesting three dimensions.

DOI: 10.1103/PhysRevB.91.035133 PACS number(s): 72.15.Rn, 64.60.ae, 03.65.Vf, 72.20.Ee

I. INTRODUCTION

Decades of studies of transport and metal-insulator transitions in disordered materials have resulted in well-established qualitative pictures of these phenomena [1–3]. The conventional wisdom prescribes that single-particle transport and localization phenomena can be understood by considering electron scattering only close to the Fermi surface; elastic scattering through states far from the Fermi surface is believed to only finitely renormalize the parameters of the low-energy excitations, without any qualitative consequences.

However, such qualitative picture is not always correct, as has been known since the pioneering works in Refs. [4–6], which showed that the transport and localization in materials with Dirac quasiparticle dispersion are qualitatively affected by elastic scattering between all states, even far from the Fermi surface. For example, in three-dimensional (3D) Dirac materials, the scattering contribution from the full band is known to lead to a disorder-driven phase transition between weak- and strong-disorder phases [5,6]. This picture has been extensively elaborated on and is now widely accepted [7–14].

In our recent paper [11], we have demonstrated [in a controlled renormalization-group (RG) analysis] that such single-particle interference far from the Fermi surface is not specific to Dirac materials; it dramatically affects transport and the metal-insulator transition in *any* semiconductor or a semimetal in *sufficiently high dimensions*. This applies, in particular, in the case of the quadratic quasiparticle dispersion in dimensions $d \geqslant 4$ and in the case of Dirac Hamiltonians in dimensions $d \geqslant 2$.

As discussed in Ref. [11], in a material with quasiparticle kinetic energy

$$\xi_{\mathbf{k}} = ak^{\alpha} \tag{1.1}$$

in the dimensions $d > d_c \equiv 2\alpha$, quasiparticle states near the bottom of the band experience renormalizations from all the other states in the band in the presence of a random short-range-correlated potential. This leads to a quantum phase transition already in the single-particle properties as a function of the disorder strength, as summarized in Fig. 1. Depending on whether the disorder strength $\varkappa$ is above or below a critical value $\varkappa_c$, the effects of quenched random potential grow or decrease at small momenta, respectively.

As a result, the density of states close to the bottom of the band exhibits a critical behavior as a function of disorder strength, unlike its smooth dependence on both energy and disorder strength in the more familiar case of $d < 2\alpha$.

A well-known example of materials corresponding to the case of $d > 2\alpha$ is the recently realized [15–19] Weyl semimetals, 3D materials with Dirac-type linear quasiparticle dispersion [20,21] ($d = 3$, $\alpha = 1$). While localization in a single-valley Weyl semimetal due to potential disorder is forbidden by symmetry [21,22], the weak-to-strong-disorder transition persists and manifests itself in, e.g., the critical behavior of the conductivity $\sigma(\varkappa) \propto |\varkappa - \varkappa_c|^{\nu(d-2)}$, that has been analyzed microscopically for small but finite doping in our recent paper, Ref. [11], and also for zero doping in Refs. [5,23,24]. The critical behavior of the density of states for 3D Dirac quasiparticles has been studied in Refs. [5,9,14,24].

As we have also demonstrated there, disordered semiconductors with the conventional quadratic quasiparticle spectrum ($\alpha = 2$) in $d > 4$ dimensions are also characterized by a critical disorder strength. Although one might think that such predictions are of purely academic interest, the properties of high-dimensional semiconductors are observable experimentally: a disordered semiconductor with a quadratic spectrum in arbitrary dimension d can be mapped [25,26] to a one-dimensional periodically kicked quantum rotor, similar to those already realized [27–29] in cold atomic gases to simulate Anderson localization in 1D and 3D. Thus such kicked rotors present a flexible experimental platform for observing the unconventional localization physics of high-dimensional semiconductors explored here. Also, our results can be tested in numerical simulations of Anderson localization transition in high dimensions [30–33] close to the band edge.

In contrast, in *subcritical* dimensions, $d < 2\alpha$, the RG analysis shows that the effects of disorder grow at smaller momenta and are most important close to the Fermi energy. This is consistent with the common assumption, widely used in the

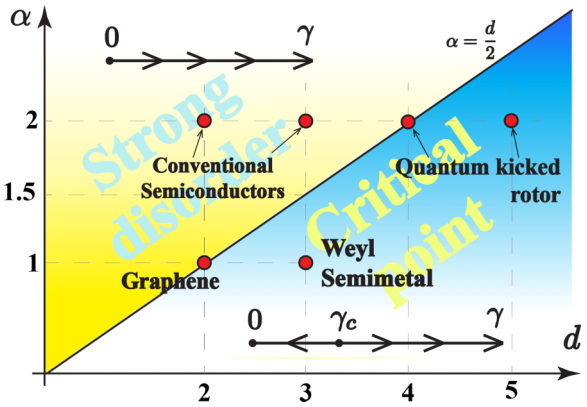

FIG. 1. (Color online) Critical behavior of weak short-correlated disorder in materials with power-law quasiparticle dispersion $\xi_{\mathbf{k}} \propto k^{\alpha}$ in dimension d. In low dimensions $d < 2\alpha$, the effects of disorder grow at small momenta (strong-disorder regime), while in high dimensions $d > 2\alpha$, there is a quantum phase transition between the strong-disorder and weak-disorder regimes. The insets show the RG flow of the dimensionless measure of the disorder strength relative to kinetic energy $\gamma(K) \sim [K\ell(K)]^{-1}$ with decreasing the characteristic momentum K, where $\ell(K)$ is the mean free path.

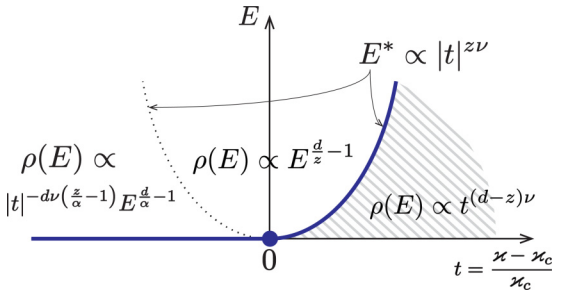

FIG. 2. (Color online) The energy (E, in the conduction band) vs disorder strength ($\varkappa$) phase diagram for a semiconductor in the orthogonal symmetry class (permitting Anderson localization) above the critical dimension, $d > 2\alpha$. The disorder-averaged density of states in different regimes is indicated. The parameter $t = \varkappa/\varkappa_c - 1$ is the deviation of the disorder strength $\varkappa$ from the critical value $\varkappa_c$. The hatched region corresponds to localized states if $d > 2$. The mobility threshold is shown as the blue curve. The dotted curve indicates a crossover from the critical to the effective disorder-free regime.

literature [1,2,34], that one may consider only quasiparticles near the Fermi surface when describing transport and metal-insulator transitions in metals and conventional semiconductors. In this paper, we further study the weak-to-strong disorder transition in materials with $d > 2\alpha$, such as high-dimensional semiconductors and semimetals, particularly focusing on the disorder-averaged density of states.

We conclude Introduction by summarizing our key results and experimental predictions. Then in Sec. II we introduce the model for a semiconductor with a power-law dispersion and short-correlated disorder. In Sec. III, we discuss the tails of the density of states that emerge below the edge of the conduction band due to rare fluctuations of the disorder potential (Lifshitz tails). In Sec. IV, we develop a perturbation theory for the states in the conduction band and obtain divergent contributions to the effective disorder strength for dimensions higher than critical. Sec. V is devoted to the RG treatment of the problem, controlled by an $\varepsilon = 2\alpha - d$ expansion. In Sec. VI, we study the disorder-averaged density of states, the mobility threshold, and the localization length using scaling analysis and complementary microscopic calculations. Section VII deals with the density of states in Weyl semimetals. We conclude in Sec. VIII with a summary and a discussion of open questions.

Summary of the results

The key features of our findings for quadratically and linearly dispersing semiconductors and Dirac semimetals is encoded in the diagram in Fig. 1. As summarized there, for $d < 2\alpha$, the effects of random potential grow at long wavelengths relative to the kinetic energy, which, if allowed by symmetry and if $d > 2$ (in addition to $d < 2\alpha$), leads to a mobility threshold between low-energy localized and high-energy delocalized states. In stark contrast, for $d > 2\alpha$, and disorder strength $\varkappa$ weaker than the critical $\varkappa_c$, the effective disorder strength decreases relative to the kinetic energy for low momenta. On the other hand, disorder stronger than critical grows at long wavelengths, leading to a finite density of states and localization (if permitted by symmetry). This leads to a disorder-driven quantum phase transition that underlies all our results.

We study this transition using scaling analysis and a complementary microscopic calculation, based on the RG analysis, controlled by

$$\varepsilon = 2\alpha - d \tag{1.2}$$

expansion, and compute a number of physical observables.

1. Density of states

We find that the density of states exhibits the critical behavior (which has been proposed previously in Ref. [14] for 3D Dirac quasiparticles)

$$\rho(E,\varkappa) = E^{\frac{d}{z}-1}\Phi\left[(\varkappa - \varkappa_c)/E^{\frac{1}{z\nu}}\right], \tag{1.3}$$

with the limiting cases summarized in Fig. 2. Here, z and ν are respectively the dynamical and the correlation length critical exponents and $\Phi[x]$ is a universal scaling function.

There are three different regimes of the critical behavior of the density of states $\rho(E,\varkappa)$.

Close to the critical disorder strength, $\varkappa \approx \varkappa_c$, the density of states is given by a power-law $\rho(E,\varkappa) \propto E^{\frac{d}{z}-1}$ and is disorder-strength-independent. For low energies and subcritical disorder ($\varkappa < \varkappa_c$), the energy dependence of the density of states coincides with that of a disorder-free system, but with a disorder-dependent enhancing prefactor that diverges as the transition is approached ($\varkappa \to \varkappa_c - 0$): $\rho(E,\varkappa) \propto (\varkappa_c - \varkappa)^{-d\nu(z/\alpha-1)} E^{d/\alpha-1}$, Fig. 3. For low energies and strong disorder ($\varkappa > \varkappa_c$), the density of states is smeared by disorder and is thus finite and only weakly energy dependent.

For a semiconductor [a material with the quasiparticle dispersion (1.1) in the orthogonal symmetry class], we find the critical exponents z and ν in the RG framework with small

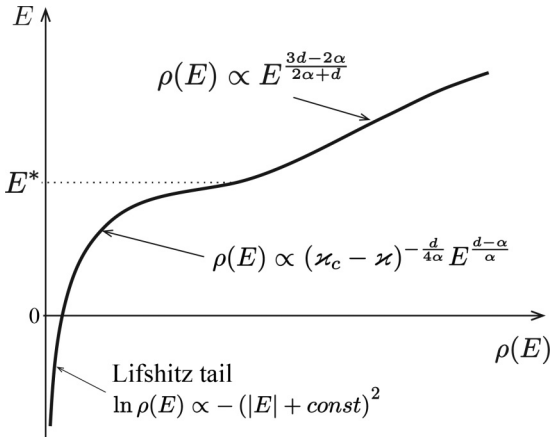

FIG. 3. The low-energy density of states in a disordered semiconductor in a dimension d above 2α for subcritical disorder strength ($\varkappa < \varkappa_c$).

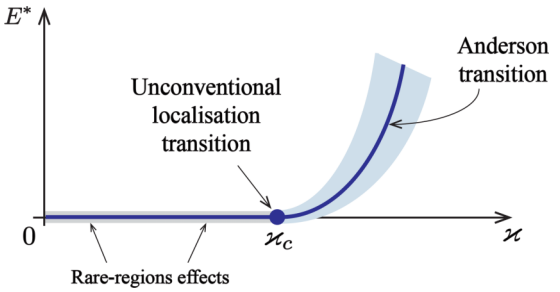

FIG. 4. (Color online) Mobility threshold $E^*(\varkappa)$ showing a non-analytic behavior [given by Eq. (1.8) close to the critical point] as a function of the disorder strength $\varkappa$ in higher dimensions ($d > 2\alpha$). In the blue (grey) wedgelike region, the critical behavior is that of the Anderson universality class with the localization length (1.7), and outside it is determined by the high-dimensional critical point ($\varkappa = \varkappa_c$, $E = 0$) studied here.

ε in the one-loop approximation:

$$\nu = -\varepsilon^{-1}, \tag{1.4}$$

$$z = \alpha - \frac{\varepsilon}{4}. \tag{1.5}$$

For instance, in the case $\alpha = 2$, $d = 5$, which can be particularly easily realized numerically, using the tight-binding model on a square lattice, and also simulated in quantum-kicked-rotor systems, Eqs. (1.4) and (1.5) give $\nu = 1$ and $z = 9/4$. We emphasize, however, that the respective $\varepsilon = -1$ is not small and may require a similar high-loop calculation to accurately describe experimentally and numerically observed values of the exponents ν and z.

Disorder not only affects the states in the conduction band of a semiconductor, but also leads to the formation of "Lifshitz tails" [35–38], deeply localized states below the edge of the conduction band that occur due to rare fluctuations of the disorder potential.

We find that the nature of the Lifshitz tail depends crucially on whether or not the dimension d is above or below critical, in the case of Gaussian disorder considered in this paper. Unlike the conventional case of low dimensions, broadly studied in the literature [35–38], for $d \geqslant 2\alpha$, the density of states just below the edge of the conduction band is exponentially suppressed at weak disorder and weakly depends on energy:

$$\rho_{\text{Lifshitz}}(0) \propto \exp\left(-\frac{A}{|\varepsilon|}\frac{\varkappa_c}{\varkappa}\right), \tag{1.6}$$

where A is a constant of order unity.

We note that the position of the band edge is shifted upon renormalization, and we define the energy E in the conduction band [cf. Eq. (1.3)], as well as Lifshitz tail relative to the renormalized edge.

Because of the exponential suppression of the tail in the limit of weak disorder or small ε, here the conduction band can be clearly distinguished from the Lifshitz tail in these limits, and the band edge is clearly defined [39]. This should be contrasted with the conventional case of low dimensions, where the contribution of the Lifshitz tail can be significant near the bottom band, and thus the band edge is not well-defined.

2. *Mobility thresholds and localization length*

Another profound consequence of single-particle interference effects in high dimensions is the unusual behavior of the mobility threshold [the energy $E^*(\varkappa)$ separating localized and delocalsed states] as a function of the disorder strength, in contrast to its conventional smooth behavior in low dimensions. Slightly above the critical dimension ($0 < -\varepsilon \ll 1$) the mobility threshold is pinned to the bottom [39] of the band for subcritical disorder, $\varkappa < \varkappa_c$, and rapidly grows with disorder strength for stronger disorder, $\varkappa > \varkappa_c$, as illustrated in Figs. 2 and 4.

Furthermore, we show that the critical properties of the localization transition in higher dimensions are richer than those below the critical dimension. According to the conventional wisdom, in the vicinity of the Anderson transition localized wave functions are characterized by a localization length that diverges at the transition as

$$\xi_{\text{loc}}(E,\varkappa) \propto |E^*(\varkappa) - E|^{-\nu_A} \tag{1.7}$$

with a finite mobility threshold E^* in the conduction band and a correlation-length exponent ν_A which is believed to be universal and to depend only on the dimension d and the symmetry class, provided the latter allows for localization. In particular, the exponent ν_A is believed to be independent of the quasiparticle dispersion in a given symmetry class.

In contrast, we find that the phenomenology in high dimensions ($d > 2\alpha$) is richer. For $\varkappa > \varkappa_c$, the critical behavior is indeed described by Eq. (1.7) with a universal exponent ν_A, but with the mobility threshold vanishing as $\varkappa$ approaches $\varkappa_c + 0$ [see also Eq. (1.3)],

$$E^*(\varkappa) = c(\varkappa - \varkappa_c)^{z\nu}, \tag{1.8}$$

and remaining zero for $\varkappa < \varkappa_c$. For $\varkappa = \varkappa_c$, however, the localization length of the $E = 0$ state diverges according to

$$\xi_{\text{loc}}(\varkappa) \propto (\varkappa - \varkappa_c)^{-\nu} \tag{1.9}$$

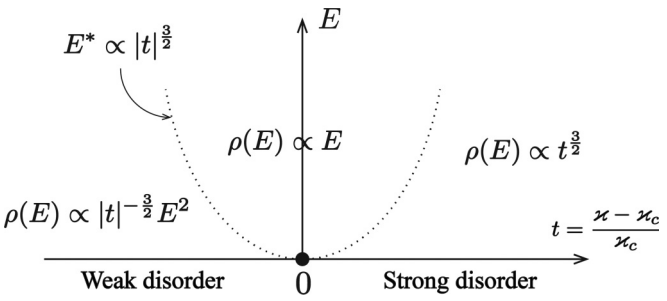

FIG. 5. The phase diagram for a disordered Weyl semimetal ($d = 3$, $\alpha = 1$) illustrating weak-to-strong-disorder phase transition at $E = 0$. Unlike a semiconductor in the orthogonal symmetry class (Fig. 2), in Weyl semimetals there are no localized states for the sufficiently smooth disorder potential under consideration. The values of the exponents in the density of states $\rho(E)$ are calculated using a perturbative one-loop RG scheme for Dirac quasiparticles, controlled by an $\varepsilon = 2 - d$ expansion.

with the universal exponent ν given by Eq. (1.4) in the limit of small ε.

Finally, for subcritical disorder, $\varkappa < \varkappa_c$, the localization length changes rapidly in a small energy interval, in which the conduction band crosses over to the Lifshitz tail. Indeed, we demonstrate that in the conduction band quasiparticle states are delocalized for $\varkappa < \varkappa_c$, because the disorder strength vanishes upon renormalization, while in the tail, the localization length is of the order of the correlation length of the potential.

3. *Weyl semimetal*

In addition to semiconductors with a scalar Hamiltonian of the kinetic energy of quasiparticles, we study the density of states in Weyl semimetal, where electrons are characterized by the Dirac-type dispersion $\hat{\mathcal{H}}(\mathbf{k}) = v\hat{\boldsymbol{\sigma}} \cdot \mathbf{k}$.

Although there is no localization in Weyl semimetal in the presence of smooth random potential, such system still exhibits the disorder-driven phase transition, manifested in, e.g., the density of states, as summarized in Figs. 5 and 6. These results are obtained using an RG approach (similar to the calculation for a semiconductor) controlled by small ε with $\varepsilon = -1$ set at the end of the calculation.

II. MODEL

As discussed in Introduction, in this paper, we study a single-particle problem in the presence of a quenched random potential and analyze the effects of the latter on the single-particle density of states and other related properties.

We consider a semiconductor with the quasiparticle Hamiltonian

$$\hat{h} = a|\mathbf{k}|^\alpha + U(\mathbf{r}) \tag{2.1}$$

in the conduction band, where $a|\mathbf{k}|^\alpha$ is the kinetic energy of a quasiparticle with momentum $\mathbf{k}$, and $U(\mathbf{r})$ is a weak Gaussian disorder potential with zero average $\langle U(\mathbf{r})\rangle_{\text{dis}} = 0$ and a correlation function

$$\langle U(\mathbf{r})U(\mathbf{r}')\rangle_{\text{dis}} = \Upsilon(\mathbf{r} - \mathbf{r}'). \tag{2.2}$$

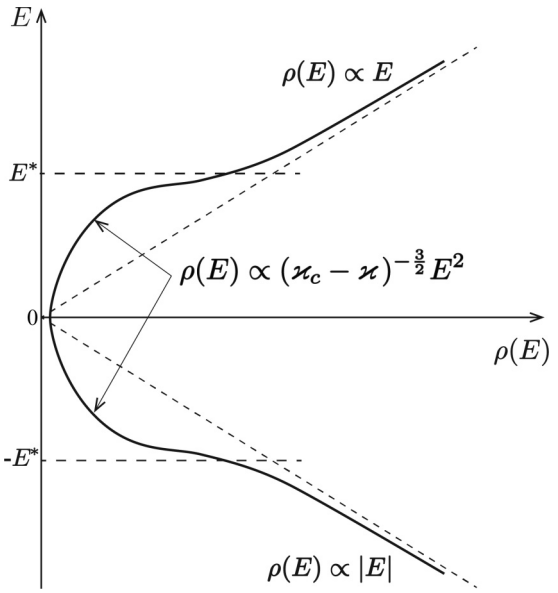

FIG. 6. The renormalized density of states in a disordered Weyl semimetal ($d = 3, \alpha = 1$) near the Dirac point for subcritical disorder. It illustrates the crossover from the linear-in-E form (controlled by the 3D critical point close to $\varkappa = \varkappa_c$ and $E = 0$) to disorder-free quadratic E^2 form at lowest energies, with a universal prefactor enhanced by disorder.

We take the latter to decay quickly on distances $|\mathbf{r} - \mathbf{r}'|$ larger than the characteristic length r_0.

If the disorder potential is caused by neutral impurities, lattice defects or vacancies, r_0 is of the order of the typical size of these impurities or defects. Disorder in semiconductors and semimetals can be represented also by screened Coulomb impurities [40], in which case r_0 is given by the screening radius. For doped semiconductors, the screening is determined by the concentration of dopants, for intrinsic semiconductors—by electrons thermally activated from the valence band or by electron and hole puddles that emerge due to the fluctuations of the impurity concentration [40–42].

In what follows, we refer to r_0 as the "impurity size." As we show in Sec. IV, the scale $K_0 = r_0^{-1}$ serves as an ultraviolet momentum cutoff for the interference effects in the conduction band, which lead to the renormalization of the states close to the bottom [39] of the band.

If processes under consideration involve momentum states with wavelengths exceeding r_0, the disorder can be considered δ-correlated,

$$\langle U(\mathbf{r})U(\mathbf{r}')\rangle_{\text{dis}} = \varkappa\delta(\mathbf{r} - \mathbf{r}'), \tag{2.3}$$

where $\varkappa = \int \Upsilon(\mathbf{r})d\mathbf{r}$.

In this paper, in the case of a semiconductor, we neglect electron scattering to the valence band, valid, for instance, in the case of a sufficiently large band gap Δ, separating the conduction and the valence bands, which exceeds the width of the conduction band or the disorder-determined ultraviolet (UV) energy cutoff aK_0^α. However, in the case of a Weyl semimetal, there is no band gap, and we therefore take into account scattering between the conduction and the valence bands.

Throughout the paper, we assume that the dimension d is integer, while the exponent α can be fractional. In particular, the parameter

$$\varepsilon = 2\alpha - d \tag{2.4}$$

can be arbitrarily small.

III. LIFSHITZ TAILS AND RARE-REGIONS EFFECTS IN HIGH DIMENSIONS

While typical fluctuations of the disorder potential can be treated in a perturbative RG analysis, discussed in the main part of the manuscript, rare regions of space with large disorder potential require more subtle nonperturbative analysis and lead to the formation of states with arbitrarily low energies E below the edge of the conduction band, known as "Lifshitz tail." Understanding the structure of such tails is indispensable for a complete description of single-particle states in disordered semiconductors.

Lifshitz tails have been extensively studied for conventional semiconductors [35–38], corresponding to low dimensions $d < 2\alpha$. For a quadratic quasiparticle dispersion, it has been estimated for the density of states $\rho(E)$ deep in the Lifshitz tail in dimension d that $\ln \rho(E) \propto -|E|^{2-d/2}$ in the case of Gaussian disorder considered in this paper (in principle, the result is nonuniversal and will differ for non-Gaussian disorder).

In what immediately follows, we use phenomenological arguments, similar to those of Refs. [35–38], to obtain the density of states in the Lifshitz tail in high dimensions, $d > 2\alpha$. We find that the structure of the tail is dramatically different from the case of low dimensions, again uncovering the crucial role played by the critical dimension $d_c = 2\alpha$. In particular, for weak disorder or small ε, the density of states $\rho(E)$ weakly depends on energy, $\ln \rho(E) \approx \ln \rho(0)$, and is exponentially small for sufficiently small energies E, including $E = 0$, which is of particular interest to us. The states with large negative energies E occur due to rare regions with large negative disorder potential that trap particle states.

The distribution of the average disorder potential $W = \frac{1}{V}\int_\Omega U(\mathbf{r})d\mathbf{r}$ in a spatial region Ω of volume $V \gg r_0^d$ is described by the Gaussian probability density

$$P_\Omega(W) = \sqrt{\frac{2\pi V}{\varkappa}} e^{-\frac{W^2 V}{2\varkappa}}, \tag{3.1}$$

as follows from Eq. (2.3).

The density of states $\rho(E)$ at a large negative energy E in a semiconductor with quasiparticle dispersion $\xi_k = ak^\alpha$ is determined by the fluctuations of the potential on length scales L that exceed the characteristic impurity size r_0 [the correlation radius of the function $\Upsilon(\mathbf{r})$]. We thus consider the contribution of such rare regions of deep random potential wells of characteristic size L to the density of states.

States with energy E and typical linear size L occur due to the potential fluctuations $W \sim -(|E| + aL^{-\alpha})$ in spatial regions of volume $\sim L^d$, where $\sim aL^{-\alpha}$ estimates the kinetic energy of the zero-point motion that raises the energy E above W, the bottom of the potential well. The density of states $\rho(E)$ is determined by the "optimal fluctuation" [35–38], i.e., the value of L, which maximizes

$$\ln P_{L^d}(E) \sim -(|E| + aL^{-\alpha})^2 L^d/\varkappa. \tag{3.2}$$

The dominant contribution to the density of states $\rho(E)$ is thus determined by the competition between large scales L, that lower the zero-point kinetic energy, and small scales L, for which potential fluctuations are more probable.

In *subcritical dimensions*, $\varepsilon \equiv 2\alpha - d > 0$, the maximum is achieved at $aL^{-\alpha} = |E|d/\varepsilon$, leading to the conventional result

$$\rho_{\text{Lifshitz}}(E) \propto \exp\left[-C|E|^{2-\frac{d}{\alpha}}\left(1+\frac{d}{\varepsilon}\right)^2\left(\frac{a\varepsilon}{d}\right)^{\frac{d}{\alpha}}\varkappa^{-1}\right], \tag{3.3}$$

where C is a constant of order unity. The density of states (3.3) has been obtained previously for conventional semiconductors [35–38].

In *high dimensions*, $d > 2\alpha$, the expression (3.2) has no maximum at finite L and grows infinitely as $L \to 0$. Thus the density of states in high dimensions is determined by the shortest microscopic length scales. The minimal scale in the model is the "impurity size" r_0. Inserting $L \sim r_0$ in Eq. (3.2), we obtain

$$\rho_{\text{Lifshitz}}(E) \propto \exp\left[-C_1\left(|E| + C_2 a r_0^{-\alpha}\right)^2 r_0^d/\varkappa\right]. \tag{3.4}$$

Equations (3.3) and (3.4) correctly describe the densities of states in low ($d < 2\alpha$) and high ($d > 2\alpha$) dimensions, respectively, provided the respective exponentials are significantly smaller than unity. While Eq. (3.3) thus applies in low dimensions only for sufficiently large negative energies $|E| \gg a^{-\frac{d}{\varepsilon}}\varkappa^{\frac{\alpha}{\varepsilon}}$, Eq. (3.4) describes the density of states in the Lifshitz tail in high dimensions for all negative energies provided the disorder is weak enough, $\varkappa \ll a^2 r_0^{-\varepsilon}$.

Our result, Eq. (3.4), thus shows that in high dimensions the density of states weakly depends on energy for $|E| \lesssim ar_0^{-\alpha}$ and decays exponentially $\rho(E) \propto \exp(-C_1|E|r_0^d/\varkappa)$ otherwise.

Gapless semiconductors. Since Eq. (3.4) applies for all energies below the bottom [39] of the band, it can be used to describe the smearing of the density of states at the degeneracy point in gapless semiconductors, i.e., materials where the conduction and the valence bands touch, such as Weyl semimetals or graphene. In these materials, there is no band gap, so the expression (3.4) can be used only for $E = 0$, i.e., in the bottom of the conduction band (the top of the valence band). Indeed, for $E = 0$, $d = 3$, and $\alpha = 1$, Eq. (3.4) gives the density of states $\rho(0)$ in a Weyl semimetal, recently obtained in Ref. [43].

IV. PERTURBATION THEORY IN THE CONDUCTION BAND

In Sec. III, we addressed the density of states below the edge of the conduction band due to *rare* fluctuations of the disorder potential. Let us now consider the states in the conduction band, where it is sufficient to consider the *typical* fluctuations of the random potential.

A. Phenomenological argument for the existence of the critical dimension $d_c = 2\alpha$

Before turning to more technical perturbative and RG analyzes, we assess of the role of quenched disorder using phenomenological scaling arguments. The importance of the random potential to a singe-particle state of momentum k can be assessed by comparing the kinetic energy ak^α with the typical fluctuation $U_{\rm rms} \sim [\varkappa k^d]^{\frac{1}{2}}$ of the (zero-mean) random potential, averaged over the volume k^{-d}, set by the de Broglie wavelength $1/k$.

For $d > 2\alpha$, the ratio $U_{\rm rms}/(ak^\alpha) = k^{d/2-\alpha}\varkappa^{1/2}/a$ [$\sim\sqrt{\gamma}$, with γ being the dimensionless measure of disorder strength, introduced in Eq. (5.12) below] vanishes with reduced momentum, which reflects the irrelevance of disorder (in RG parlance) in higher dimensions.

In contrast, for $d < 2\alpha$, the effects of disorder grow at small momenta. For $d > 2$ (in addition to $d < 2\alpha$), we expect the localization of particles with sufficiently low momenta $k \lesssim K^*$, such that the kinetic energy $a(K^*)^\alpha$ is of the order of the characteristic disorder potential fluctuation $U_{\rm rms}(K^*)$. This allows us to estimate the mobility threshold in lower dimensions:

$$E_{\rm mob} \sim a^{1-2\alpha/\varepsilon}\varkappa^{\alpha/\varepsilon}. \tag{4.1}$$

Although the above phenomenological argument allows one to predict the existence of the critical dimension $d_c = 2\alpha$ and qualitatively different effects of disorder in dimensions $d > 2\alpha$ and $d < 2\alpha$, such argument neglects elastic scattering of the states with characteristic momentum k through the states $K \gg k$.

We show below that such large-momentum scattering is important in higher dimensions, but may be neglected in the dimensions below critical. Indeed, sufficiently below the critical dimension [in the limit $\varepsilon \gg \varkappa/(a^2K_0^\varepsilon)$], the phenomenological estimate (4.1) of the mobility threshold is accurate and coincides with the result [Eq. (6.20) below] of a rigorous RG calculation. However, when approaching the critical dimension ($\varepsilon \to 0$), the above estimate, Eq. (4.1), is no longer accurate, as elastic scattering between all states in the band needs to be taken into account.

B. Perturbative correction to the disorder strength

In what immediately follows, we apply perturbation theory to show that sufficiently below critical dimensions, $2\alpha - d \gtrsim 1$, the quasiparticle transport in a weakly disordered semiconductor is dominated by the scattering between states in a narrow momentum shell, $|k - K| \ll k$, whereas close to or above the critical dimensions, $d > 2\alpha$, scattering in a large band of momenta $k < K_0$, up to the UV cutoff K_0, is important.

In the leading order in the disorder strength, the effect of large-momentum scattering ($|k - K| \gtrsim k$) on states with small momenta k can be illustrated by the renormalization of the impurity line, Fig. 7, mimicked diagramatically in Fig. 8 and estimated as

$$\delta\Upsilon(\sim k) \sim 4\int_{K\gtrsim k} \frac{\Upsilon^2(\mathbf{K})}{\xi_{\mathbf{K}}^2}\frac{d^d\mathbf{K}}{(2\pi)^d}, \tag{4.2}$$

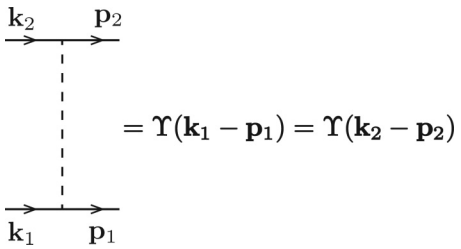

FIG. 7. Impurity line.

where $\Upsilon(\mathbf{K})$ is the Fourier transform of the disorder correlation function $\Upsilon(\mathbf{r})$, Eq. (2.3), and $\xi_{\mathbf{K}} = aK^\alpha$ is the kinetic energy of a quasiparticle with momentum $\mathbf{K}$.

For short-correlated disorder, which we consider in this paper, the function $\Upsilon(\mathbf{K})$ decays fast beyond the cutoff momentum $K_0 = r_0^{-1}$, and the renormalization of the impurity line can be rewritten in terms of modification of the disorder strength $\varkappa$, Eq. (2.3),

$$\delta\varkappa \sim 4C_d\frac{\varkappa^2}{a^2}\int_k^{K_0}\frac{dK}{K^{2\alpha-d+1}}, \tag{4.3}$$

where $C_d = S_d/(2\pi)^d$ and S_d is the area of a unit sphere in a d-dimensional space.

1. Subcritical dimensions

Consistent with the phenomenological analysis of Sec. IV A, in the dimensions $d < 2\alpha$ the integral in Eq. (4.3) is dominated by momenta $K \sim k$ near the lower limit, and

$$\delta\varkappa \sim \frac{1}{2\alpha - d}\frac{\varkappa}{k\ell(k)}, \tag{4.4}$$

where we have introduced the quasiparticle mean free path (cf. Appendix A for a detailed calculation of the mean free path)

$$\ell(k) = \frac{\alpha^2a^2k^{2\alpha-d-1}}{2\pi C_d\varkappa}. \tag{4.5}$$

The quantity $k\ell(k)$, entering Eq. (4.4), is an important parameter in the conventional Anderson localization theory in the dimensions d (sufficiently) above 2. If this parameter is large, $k\ell(k) \gg 1$, the respective states are delocalized, according to the so-called Ioffe-Regel criterion [44,45]. Otherwise, $k\ell(k) \sim 1$, and the respective states are either localized and do not contribute to transport or are close to localization. In $d \leqslant 2$, all states are localized.

Conventional semiconductors in 2D and in 3D are characterized by quadratic quasiparticle spectrum ($\alpha = 2$), Fig. 1, and thus correspond to the dimensions below critical, $2\alpha - d \gtrsim 1$.

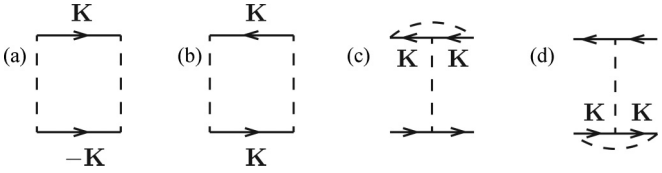

FIG. 8. The leading-order diagrams for the renormalization of the impurity line due to scattering through states with large momenta. Large momentum $\mathbf{K}$ significantly exceeds the other incoming and outgoing momenta. Diagrams (a)–(d) have equal values.

Then Eq. (4.4) shows that for states with $k\ell(k) \gg 1$, the large-momentum scattering produces only small corrections to the disorder strength $\delta\varkappa \sim \varkappa/[k\ell(k)]$ and can be neglected.

Thus, in conventional semiconductors, one can apply the usual transport theory and disorder-averaging techniques [1], with quasiparticle scattering confined inside a small momentum shell near the Fermi surface and neglecting the other states in the band.

2. *Dimensions close to or above critical*

When approaching the critical dimension, $d \to 2\alpha$, the renormalization of the disorder strength (4.4) by interference processes involving large momenta dramatically increases. In the dimensions $d > 2\alpha$, the integral in Eq. (4.4) is dominated by large momenta close to the ultraviolet cutoff $K_0 = r_0^{-1}$;

$$\delta\varkappa = 4C_d \frac{\varkappa^2}{a^2} \frac{1}{d-2\alpha} \frac{1}{r_0^{d-2\alpha}}. \tag{4.6}$$

The modification of the disorder strength by processes involving momenta $\sim K_0$ can become very large and diverges in the limit of δ-correlated disorder $r_0 \to 0$. Such effects cannot be treated perturbatively and require adequate renormalization-group analysis, to which we turn in the next section.

V. RENORMALIZATION GROUP ANALYSIS

In order to address the effects of random potential beyond the above phenomenological and perturbative approaches, in this section, we develop a logarithmic renormalization-group description for the states in the conduction band in the critical dimension $d = 2\alpha$ and address the other dimensions by means of an

$$\varepsilon = 2\alpha - d \tag{5.1}$$

expansion.

Similar renormalization-group descriptions have been developed for systems with Dirac-type quasiparticle dispersion in two and three dimensions (2D and 3D), such as the Ising model [4], integer-Hall-effect systems [7], d-wave superconductors [8], topological insulators [9], graphene [10], and Weyl semimetals [5,6,11].

For concreteness and because of its central role in characterising the system, we focus on the disorder-averaged single-particle density of states

$$\rho(E) = -\frac{1}{\pi} \mathrm{Im} \left\langle \frac{1}{V} \int d\mathbf{r}\, G^R(\mathbf{r},\mathbf{r},E) \right\rangle_{\mathrm{dis}} \tag{5.2}$$

in the conduction band, where $\langle G^R(\mathbf{r},\mathbf{r}',E)\rangle_{\mathrm{dis}}$ is the disorder-averaged retarded Green's function. In the supersymmetric representation [2] (here used as a convenient tool, although Keldysh and replica representations can be equivalently utilized),

$$\langle G^R(\mathbf{r},\mathbf{r},E)\rangle_{\mathrm{dis}} = -i \int \mathcal{D}\psi\mathcal{D}\psi^\dagger e^{-\mathcal{L}_0-\mathcal{L}_{\mathrm{int}}} s(\mathbf{r})s^*(\mathbf{r}), \tag{5.3}$$

$$\mathcal{L}_0 = -i \int \psi^\dagger [E + i0 - a|\hat{k}|^\alpha]\psi \, d\mathbf{r}, \tag{5.4}$$

$$\mathcal{L}_{\mathrm{int}} = \frac{1}{2}\varkappa \int (\psi^\dagger\psi)^2 d\mathbf{r}, \tag{5.5}$$

where $\psi = (\chi, s)^T$ and $\psi^\dagger = (\chi^*, s^*)$ are a row and a column of anticommuting (Grassman) χ, χ^* and commuting s, s^* fields, and $\hat{k} = -i\partial_{\mathbf{r}}$.

In Eq. (5.5), we have taken the random potential to be zero-mean and δ-correlated, as the low-energy states under consideration are smooth on the scale $r_0 = K_0^{-1}$. Integrating out the modes with the highest momenta in an infinitesimal shell $Ke^{-l} < k < K$ leads to a modified expression for the density of states:

$$\rho(E) = \frac{1}{\pi V} \mathrm{Re} \left[\lambda(K) \int \mathcal{D}\psi\mathcal{D}\psi^\dagger d\mathbf{r}\, e^{-\tilde{\mathcal{L}}_0-\tilde{\mathcal{L}}_{\mathrm{int}}} s(\mathbf{r})s^*(\mathbf{r}) \right] \tag{5.6}$$

with a renormalized Lagrangian $\tilde{\mathcal{L}}_0 + \tilde{\mathcal{L}}_{\mathrm{int}}$,

$$\tilde{\mathcal{L}}_0 = -i \int \psi^\dagger [\lambda(K)(E + i0) - a|\hat{k}|^\alpha]\psi \, d\mathbf{r}, \tag{5.7}$$

$$\tilde{\mathcal{L}}_{\mathrm{int}} = \frac{1}{2}\tilde{\varkappa}(K) \int (\psi^\dagger\psi)^2 d\mathbf{r}, \tag{5.8}$$

where the resulting effective couplings $\lambda(K)$ and $\tilde{\varkappa}(K)$ flow as

$$\partial_l \lambda = \frac{C_d}{a^2} \tilde{\varkappa}\lambda K^{-\varepsilon}, \tag{5.9}$$

$$\partial_l \tilde{\varkappa} = \frac{4C_d}{a^2} \tilde{\varkappa}^2 K^{-\varepsilon}, \tag{5.10}$$

with the initial values $\tilde{\varkappa}(K_0) = \varkappa$ and $\lambda(K_0) = 1$ (for a detailed derivation of the RG equations see Appendix B).

The renormalized Lagrangian retains the δ-correlated disorder form,

$$\langle U(\mathbf{r})U(\mathbf{r}')\rangle = \tilde{\varkappa}(K)\delta(\mathbf{r} - \mathbf{r}'), \tag{5.11}$$

with $\tilde{\varkappa}(K)$ characterising the renormalized disorder strength. The parameter $\lambda(K)$ plays the role of the inverse quasiparticle weight.

We note that the edge of the conduction band also flows under the RG. Thus, throughout the paper, the energy E is implicitly understood to be measured from the renormalized band edge.

The form of the flow equations (5.9) and (5.10) for dimensionful couplings suggests an introduction of a dimensionless measure of disorder strength

$$\gamma(K) = \frac{4C_d}{a^2} \tilde{\varkappa}(K) K^{-\varepsilon}, \tag{5.12}$$

in terms of which the RG equations reduce to a simple form:

$$\partial_l \lambda = \gamma\lambda/4, \tag{5.13}$$

$$\partial_l \gamma = \varepsilon\gamma + \gamma^2. \tag{5.14}$$

The RG equations (5.13) and (5.14) are similar to those for systems with Dirac-type quasiparticle dispersion, extensively studied in the literature [4–11,13,46]. We discuss the RG equations for such Dirac materials and the critical behavior, that follows from them, in Sec. VII.

We note that the dimensionless parameter $\gamma(k)$ is related to the mean free path $\ell(k)$, Eq. (4.5) as

$$\gamma(k) = \frac{2\alpha^2}{\pi}\frac{1}{k\ell(k)} \tag{5.15}$$

and is also a square of the ratio $U_{\rm rms}(k)/(ak^\alpha)$ of the rms value of the random potential to the kinetic energy at momentum k (see Sec. IV A). In realistic system $\alpha \sim 1$, so $\gamma(k)$ is of the order of the parameter [44,45] $[k\ell(k)]^{-1}$, which plays an important role [1,2,34] in the studies of disordered metals and semiconductors.

Thus, the parameter $\gamma(K)$ reflects the localization properties of the states with momenta of the order of K in $d > 2$ dimensions (cf. also Appendix A). Namely, according to the Ioffe-Regel criterion (and as supported by detailed microscopic calculations [2,3]), the state with energy E is delocalized if $\gamma(K_E) \ll 1$ with K_E given by Eq. (5.16). If disorder grows upon renormalization, the mobility threshold is reached at the value of the momentum cutoff K, such that $\gamma(K) \sim 1$.

Termination of the RG. To utilize our RG approach for a computation of a physical quantity at energy E [e.g., the density of states $\rho(E)$], we stop integrating out high-momentum modes when the momentum cutoff K reaches an E-dependent value K_E, such that

$$\lambda(K_E)E \sim aK_E^\alpha, \tag{5.16}$$

as determined by the quadratic part of the Lagrangian, Eq. (5.7).

On the other hand our RG approach is perturbative in the dimensionless disorder strength γ and is thus only valid for $\gamma \ll 1$. This therefore places a condition ($E > E^*$) on the minimum energy that can be studied within this analysis in a regime where disorder is relevant at low energies.

The RG procedure must also be terminated if the density of states $\rho(E)$, derived from Eqs. (5.6)–(5.8), becomes smaller than the density of states $\rho_{\rm Lifshitz}(0)$ in the Lifshitz tail near the edge of the band, emerging due to rare strong fluctuations of the disorder potential. Indeed, the latter occur as instantons in the disorder-averaged quasiparticle action [47,48] and thus cannot be taken into account by a perturbative RG procedure. If the instanton contribution to the density of states dominates, the contributions from the typical disorder fluctuations are no longer important.

In high dimensions $d > 2\alpha$ the density of states (3.4) in the Lifshitz tail does not experience renormalizations from the interference effects in the conduction band, because it originates from rare fluctuations of the random potential on the scale of the disorder correlation length r_0, i.e., from the momentum modes close to the ultraviolet cutoff K_0. However, the density of states (3.3) just below the critical dimensions, $0 < 2\alpha - d \ll 1$, is subject to renormalizations.

Critical point. Below critical dimensions ($\varepsilon > 0$), $\gamma(l)$ always flows to larger values, according to Eq. (5.14). This encodes the conventional wisdom that the effective random potential becomes stronger at the bottom [39] of the band. For $2 < d < 2\alpha$, this is consistent with the usual expectation of the existence of a mobility edge that evolves smoothly in the conduction band as a function of disorder strength.

In qualitative contrast to this conventional expectation, for supercritical dimension, $d > 2\alpha$, $\gamma(l)$ is irrelevant, flowing to the $\gamma = 0$ disorder-free Gaussian fixed point for γ smaller than the critical value

$$\gamma_c = -\varepsilon, \tag{5.17}$$

in accordance with the phenomenological analysis of Sec. IV A. Instead, for disorder strength exceeding the critical γ_c, $\gamma(l)$ flows to larger values, reflecting the relevance of strong disorder in higher dimensions. These two regimes are then separated by a critical fixed point γ_c.

Thus, for $d > 2\alpha$ ($\varepsilon < 0$), the renormalization flow leads to a disorder-driven quantum phase transition. Namely, the effects of the random potential on the states near the edge of the band may be significant or negligible depending on whether or not the disorder strength $\varkappa$ exceeds the critical value

$$\varkappa_c = -\varepsilon\frac{K_0^\varepsilon a^2}{4C_d}. \tag{5.18}$$

Below, we show how this transition manifests itself in the density of states near the edge of the band and the position of the mobility threshold.

Solution of the RG equations. The RG flow equations (5.9) and (5.10) [(5.13) and (5.14)] can be solved exactly [11] with the result

$$\tilde\varkappa(K) = \frac{\varkappa}{1 - \frac{\varkappa}{\varkappa_c} + \frac{\varkappa}{\varkappa_c}\left(\frac{K_0}{K}\right)^\varepsilon}, \tag{5.19}$$

$$\lambda(K) = [\tilde\varkappa(K)/\varkappa]^{1/4}. \tag{5.20}$$

If the renormalization procedure is terminated at weak disorder, $\gamma \ll 1$, the action (5.6)–(5.8) with renormalized parameters (5.19) and (5.20) can be used to compute low-energy physical observables, such as conductivity [11] and the density of states, evaluated in the next section.

VI. DENSITY OF STATES AND MOBILITY THRESHOLD

A. Scaling analysis for the density of states

The existence of the critical point in a semiconductor [material with quasiparticle dispersion (1.1) in the orthogonal symmetry class] in $d > 2\alpha$ dimensions suggests that the density of states exhibits a critical behavior near this point. Such behavior is dramatically different from the conventional case of low dimensions ($d < 2\alpha$), where the critical point is absent and the disorder-averaged density of states and mobility threshold is known to be a smooth function of the disorder strength [2,31,49].

In what immediately follows, we use general scaling arguments to describe the density of states near the critical point. In the next sections, we confirm this critical behavior by a microscopic calculation in the limit of small ε.

According to the conventional phenomenology, near a continuous transition one expects the existence of a single dominant correlation length scale

$$\xi(\varkappa, E) = E^{-\frac{1}{z}} g\left[(\varkappa - \varkappa_c)/E^{\frac{1}{z\nu}}\right], \tag{6.1}$$

where ν and z are the correlation-length and dynamical critical exponents respectively, and the energy E is measured from

the renormalized edge of the band [39]. For small energies [$E \ll E^* = c(\varkappa - \varkappa_c)^{z\nu}$] and supercritical disorder ($\varkappa > \varkappa_c$) it diverges as

$$\xi(\varkappa) \propto |\varkappa - \varkappa_c|^{-\nu}. \tag{6.2}$$

We note that, in contrast, the transition across a nonzero energy E^* (mobility threshold) is described by the conventional-Anderson-transition critical behavior, where a distinct localization length $\xi_{\rm loc} \propto |E - E^*(\varkappa)|^{-\nu_A}$ diverges, while the correlation length ξ remains finite, see Fig. 4. Finally, sufficiently close to the critical point ($\varkappa \approx \varkappa_c$),

$$\xi \propto E^{-\frac{1}{z}}. \tag{6.3}$$

Following the conventional paradigm [50], near critical point physical quantities are expected to be expressible in terms of this divergent correlation length. According to this, we expect the density of states to have the scaling dimensions of density over energy, $\rho \sim \xi^{-d}/E$, and thus to exhibit the form

$$\rho(E,\varkappa) = E^{\frac{d}{z}-1}\Phi\left[(\varkappa - \varkappa_c)/E^{\frac{1}{z\nu}}\right] + \rho_{\rm smooth}, \tag{6.4}$$

where $\Phi(x)$ is a universal scaling function. Here, $\rho_{\rm smooth}$ is an analytic contribution to the density of states in the conduction band, derived from the same rare-regions effects as the Lifshitz tail. In what follows, we consider the states in the conduction band and neglect the latter nonperturbative instantonic contribution, Eq. (3.4), since it is suppressed by sufficiently large energy E and small ε.

Based on Eq. (6.4) we expect that close to the critical disorder strength, $\varkappa \approx \varkappa_c$, $\Phi(x \to 0) \to$ const and the density of states near the edge of the band depends on the energy as

$$\rho(E) \propto E^{\frac{d}{z}-1}. \tag{6.5}$$

If the disorder is stronger than critical, $\varkappa > \varkappa_c$, the states with sufficiently small energies are localized, and their density is smeared by disorder. Requiring that the density of states is energy-independent dictates that in this limit $\Phi(x) \to x^{z\nu(d/z-1)}$, leading to a prediction of

$$\rho_{\rm strong} \propto (\varkappa - \varkappa_c)^{(d-z)\nu}. \tag{6.6}$$

For subcritical disorder, $\varkappa < \varkappa_c$ the dimensionless disorder strength flows to smaller values under the RG, leading the absence of localization in the conduction band (provided $d > 2$ in addition to $d > 2\alpha$). The density of states vanishes when approaching the (renormalized) edge of the band (until the Lifshitz tail is reached), but may depend on the strength of disorder. Assuming that the disorder $\tilde{\varkappa}(K)$ strength and the parameter $\lambda(K)$ in the renormalized Lagrangian (5.7) saturate at constant values as $K \to 0$ [as is also supported by the microscopic RG analysis, cf. Eqs. (5.19) and (5.20)], we expect the resulting energy dependence of the density of states to be given by the disorder-free expression $\propto E^{\frac{d-\alpha}{\alpha}}$. This requires that the scaling function in this regime has the form $\Phi(x) \propto |x|^{-d\nu(z/\alpha-1)}$, which from Eq. (6.4) then gives

$$\rho(E,\varkappa) \propto (\varkappa_c - \varkappa)^{-d\nu(\frac{z}{\alpha}-1)} E^{\frac{d-\alpha}{\alpha}}. \tag{6.7}$$

In this regime, the density of states thus exhibits a universal prefactor, that singularly enhances the disorder-free density of states, diverging as the transition at $\varkappa = \varkappa_c$ is approached from below. The three regimes, described by Eqs. (6.5)–(6.7), are summarized in Fig. 2.

B. Scaling analysis for the mobility threshold

In the previous section and in Sec. VI A, using scaling and a detailed RG analysis, we have found that for $d > d_c$ and subcritical disorder strength $\varkappa < \varkappa_c$, the effective disorder strength vanishes at low energies, and all states in the conduction band remain extended. Thus, for $\varkappa < \varkappa_c$, we expect the mobility threshold to be stuck inside or just above the Lifshitz tail, and in the $\varepsilon \to 0$ limit pinned to the bottom [39] of the conduction band.

In contrast, if the disorder is stronger than critical, the disorder strength flows to larger values, leading to the localization of states with sufficiently small energies. If the energy is not sufficiently small, the RG flow may be terminated while the disorder is still weak, leading to the absence of localization.

Thus, for $\varkappa > \varkappa_c$, we predict the existence of a finite mobility threshold $E^*(\varkappa)$ in the conduction band that separates localized and delocalized states. According to the scaling theory, we predict the mobility threshold, $E^* \propto \xi^{-z}$, to have the universal scaling form

$$E^*(\varkappa) \propto (\varkappa - \varkappa_c)^{z\nu}. \tag{6.8}$$

According to the scaling hypothesis, the energy scale E^*, Eq. (6.8), also happens to be the characteristic energy scale at which the high-energy density of states (6.5) for $\varkappa < \varkappa_c$ crosses over to the density of states (6.7) in the effective disorder-free regime, see Fig. 2.

C. Scaling analysis for the localization length

We first note that the correlation length $\xi(E,\varkappa)$, Eq. (6.1), of the state with energy E for disorder strength $\varkappa$ in general should be contrasted with the localization length $\xi_{\rm loc}(E,\varkappa)$ near the Anderson transition [near the mobility threshold $E = E^*(\varkappa)$], studied in this section.

Because for $\varkappa = \varkappa_c$ the Anderson transition occurs at zero energy, the two localization lengths, $\xi_{\rm loc}$ and ξ, are proportional to each other near the critical point ($\varkappa = \varkappa_c$, $E = 0$). This allows us to develop a scaling theory, similar to that of Sec. VI A, for the localization length

$$\xi_{\rm loc}(E,\varkappa) = (\varkappa - \varkappa_c)^{-\nu} h\left[(\varkappa - \varkappa_c)/E^{\frac{1}{z\nu}}\right], \tag{6.9}$$

where $h(x)$ is a universal scaling function.

Close to the critical point ($\varkappa = \varkappa_c$, $E = 0$), the scaling of the localization length for sufficiently-low-energy states [$E \ll c(\varkappa - \varkappa_c)^{-\nu}$] is thus given by Eq. (6.2) for disorder close to critical. However, for $\varkappa > \varkappa_c$ and as $E \to E^*(\varkappa)$, the critical behavior of the localization length is of the Anderson-transition universality class [see Eq. (1.7)], with the correlation length ξ remaining finite. This dictates the following $\varkappa \geqslant \varkappa_c$ form of the localization length:

$$\begin{aligned}\xi_{\rm loc}(\varkappa,E) &\propto (\varkappa - \varkappa_c)^{-\nu}\left[\frac{E}{(\varkappa - \varkappa_c)^{z\nu}} - c\right]^{-\nu_A} \\ &= (\varkappa - \varkappa_c)^{\nu(z\nu_A - 1)}[E - c(\varkappa - \varkappa_c)^{z\nu}]^{-\nu_A},\end{aligned} \tag{6.10}$$

where ν_A is the correlation-length exponent of the Anderson transition. Equation (6.10) holds for energies in the vicinity of

the mobility threshold $E^*(\varkappa) = c(\varkappa - \varkappa_c)^{z\nu}$, within the blue (grey) wedge-shaped region in Fig. 4.

We emphasize that the divergence of the localization length is characterized by different critical exponents at the (high-dimensional) critical point $\varkappa = \varkappa_c$, $E = 0$ and at $\varkappa > \varkappa_c$, $E = E^*(\varkappa)$. Indeed, at the former, the correlation-length and dynamical exponents are given by ν and z, respectively, while for $\varkappa > \varkappa_c$, by ν_A and [51,52] $z_A = d$.

The localization transition for subcritical disorder ($\varkappa < \varkappa_c$) occurs in a narrow interval of energies close to the bottom of the band, where the states cross over to the Lifshitz tail. Expecting that the nature of such transition is thus affected by rare regions strong-disorder effects, we leave it for future studies. In what follows, we complement the above scaling analysis by a microscopic derivation of Eqs. (6.5)–(6.8) and compute the critical exponents ν and z and the associated scaling functions microscopically in the limit of small $\varepsilon = d - 2\alpha < 0$.

D. Microscopic calculation of the density of states and mobility threshold in high dimensions, $d > 2\alpha$

In the absence of disorder, the density of states in the conduction band is given by

$$\rho_{\text{clean}}(E) = \frac{C_d E^{\frac{d-\alpha}{\alpha}}}{\alpha a^{\frac{d}{\alpha}}}, \tag{6.11}$$

and the Lifshitz tail is absent.

In the presence of disorder, the density of states $\rho(E)$ can be calculated microscopically from the renormalized Lagrangian, Eqs. (5.6)–(5.8), with the cutoff K_E, determined by Eq. (5.16). Provided the renormalized disorder remains weak, $\gamma(K_E) \ll 1$, this can be done in a controlled perturbative expansion in $\gamma(K_E)$, with the lowest-order contribution given simply by the quadratic part of the Lagrangian, Eq. (5.7), utilizing the renormalized parameters $\varkappa(K_E)$ and $\lambda(K_E)$, Eqs. (5.19) and (5.20).

To this leading order in $\gamma(K_E)$, we thus find

$$\rho(E,\varkappa) = \lambda(K_E)\,\rho_{\text{clean}}[\lambda(K_E)E] \tag{6.12a}$$

$$= \frac{C_d}{\alpha a^{\frac{d}{\alpha}}}[\lambda(K_E)]^{\frac{d}{\alpha}} E^{\frac{d-\alpha}{\alpha}} \tag{6.12b}$$

$$= \frac{C_d}{\alpha a^{\frac{d}{\alpha}}}\left[1 - \frac{\varkappa}{\varkappa_c} + \frac{\varkappa}{\varkappa_c}\left(\frac{K_0}{K_E}\right)^{\varepsilon}\right]^{-\frac{d}{4\alpha}} E^{\frac{d-\alpha}{\alpha}}, \tag{6.12c}$$

where the momentum K_E, at which the RG flow is terminated, is a function of energy E, determined by the condition

$$E\left[1 - \frac{\varkappa}{\varkappa_c} + \frac{\varkappa}{\varkappa_c}\left(\frac{K_0}{K_E}\right)^{\varepsilon}\right]^{-\frac{1}{4}} \sim aK_E^{\alpha}, \tag{6.13}$$

as follows from Eqs. (5.16), (5.19), and (5.20).

Because the disorder strength $\tilde{x}(K)$ always increases under the RG flow, according to Eq. (5.10), the parameter $\lambda(K)$ is always larger than unity. Therefore, the low-energy density of states (6.12b) in a disordered system exceeds that (6.11) in a disorder-free system. Thus impurities have transferred states from high energies $E > aK_0^{\alpha}$ to lower energies.

Examining Eqs. (6.12c) and (6.13) it is clear that the density of states exhibits three qualitatively different regimes, distinguished by the range of the momentum cutoff K_E (or correspondingly energy E) and on whether the disorder is stronger or weaker than critical.

Indeed, comparing the terms $1 - \varkappa/\varkappa_c$ and $(\varkappa/\varkappa_c)(K_0/K_E)^{\varepsilon}$ in Eqs. (6.12c), (6.13), (5.19), and (5.20) suggests an introduction of the momentum scale

$$K^* = K_0\left|1 - \frac{\varkappa_c}{\varkappa}\right|^{-\frac{1}{\varepsilon}} \tag{6.14}$$

and the corresponding energy scale $E^* = a(K^*)^{\alpha}/\lambda(K^*)$ given by

$$E^* = aK_0^{\alpha}\left|1 - \frac{\varkappa_c}{\varkappa}\right|^{\frac{1}{4} - \frac{\alpha}{\varepsilon}}. \tag{6.15}$$

The three regimes are defined by the energy E and disorder strength: (1) disorder close to critical, $\varkappa \approx \varkappa_c$, corresponding to the energy range, such that $K^* \ll K_E < K_0$; (2) subcritical disorder and low energies, $\varkappa < \varkappa_c$ and $K_E \ll K^*$; (3) supercritical disorder and low energies, $\varkappa > \varkappa_c$ and $K_E \ll K^*$.

The analysis of whether corresponding energy-E states are localized can be carried out similarly to the case of a usual metal [2]. In $d \leqslant 2$ dimensions, all the states are localized. In the dimensions $d > 2$, there is a mobility threshold E^*, corresponding to $K_{E^*}\ell(K_{E^*}) \sim 1$ [$\gamma(K_{E^*}) \sim 1$], that separates localized and delocalized states. In what immediately follows, we compute the density of states in these three regimes.

1. Critical disorder

In the case of disorder close to critical, $\varkappa \approx \varkappa_c$, corresponding to the interval of energies $E^* \ll E < aK_0^{\alpha}$, Eq. (6.11), relating the momentum K_E to the energy E, simplifies to

$$K_E = K_0\left(\frac{E}{aK_0^{\alpha}}\right)^{\frac{4}{4\alpha-\varepsilon}}. \tag{6.16}$$

This, together with Eq. (6.12c), yields the critical density of states in this energy interval

$$\rho(E) \sim \frac{C_d K_0^{d-\alpha}}{\alpha a}\left(\frac{E}{aK_0^{\alpha}}\right)^{\frac{3d-2\alpha}{2\alpha+d}}. \tag{6.17}$$

For energies of the order of or larger than the ultraviolet cutoff, $E \gtrsim aK_0^{\alpha}$, the density of states crosses over to that of a clean semiconductor, Eq. (6.11).

2. Subcritical disorder

In this regime of $\varkappa < \varkappa_c$, defined by $K_E < K^*$, the system is sufficiently away from the critical disorder strength $\varkappa_c$, so that $\frac{\varkappa}{\varkappa_c}(\frac{K_0}{K_E})^{\varepsilon}$ in Eqs. (6.12c) and (6.13) can be neglected in comparison with $1 - \varkappa/\varkappa_c$. Equation (6.12c) then immediately gives

$$\rho(E) = \frac{C_d}{\alpha a^{\frac{d}{\alpha}}}\left(1 - \frac{\varkappa}{\varkappa_c}\right)^{-\frac{d}{4\alpha}} E^{\frac{d-\alpha}{\alpha}}, \tag{6.18}$$

a result that applies for subcritical disorder and sufficiently low energies $E \ll E^*$, as illustrated in Fig. 2. The disorder-averaged low-energy density of states is asymptotically that of a disorder-free semiconductor, with the only effect of the

random potential to enhance the density of states through a universal multiplicative prefactor, that diverges near the critical point. For weak disorder, $\varkappa \ll \varkappa_c$ the renormalization is weak, and the density of states (6.18) is close to that (6.11) of a clean semiconductor.

3. *Supercritical disorder*

For disorder stronger than critical, $\varkappa > \varkappa_c$, the dimensionless measure of disorder $\gamma(K) \sim [k\ell(k)]^{-1}$ grows upon renormalization. It reaches values of order unity at momentum cutoff $K_E \sim K^*$, below which our perturbative (in γ) RG is no longer trustworthy.

However, one can apply phenomenological arguments of Sec. IV A with the renormalized strength of disorder $\varkappa^* \sim a^2(K^*)^\varepsilon$ at the RG breakdown point ($\gamma \sim 1$). At this point, the root mean square $U^*_{\rm rms} \sim [\varkappa^*(K^*)^d]^{\frac{1}{2}}$ of the renormalized random potential is comparable to the kinetic energy $a(K^*)^\alpha$. Therefore we expect that the states with energy $E < E^*$, where E^* is given by Eq. (6.15), are strongly influenced by such strong random potential and are thus localized. Conversely, for $E > E^*$ and $d > 2$, the random potential is a small perturbation and the states are delocalized.

Given that $\gamma \sim [k\ell(k)]^{-1}$ [see Eq. (5.12)], this conclusion is also consistent with the Ioffe-Regel criterion of localization (supported by rigorous analytic calculations [2,3]). We thus conclude that for $d > d_c$ the energy scale $E^*(\varkappa)$, Eq. (6.15), defines the mobility threshold for the strong disorder regime $\varkappa > \varkappa_c$, separating localized and delocalized states (so long as $d > 2$), as illustrated in Figs. 2 and 4. Because the disorder is strong for states with energies $E < E^*$, the density of states is energy-independent and is determined by the amplitude of the disorder potential fluctuations.

From Eqs. (6.12c) and (6.14), we obtain the density of states for $\varkappa > \varkappa_c$ in the energy interval $0 < E \lesssim E^*$:

$$\rho(E) \sim \frac{C_d K_0^{d-\alpha}}{\alpha a} \left(\frac{\varkappa - \varkappa_c}{\varkappa}\right)^{\frac{3}{4}-\frac{\alpha}{\varepsilon}}. \tag{6.19}$$

E. Subcritical dimensions, $d < 2\alpha$

Below critical dimensions ($\varepsilon > 0$), the disorder strength grows with decreasing energy E, appearing to diverge as K_E approaches K^*. The dimensionless measure of disorder, $\gamma(K)$ reaches values of order unity at momentum cutoff $K_{\rm mob} = K^*[1 + |\varkappa_c|/\tilde{\varkappa}(K)]^{1/\varepsilon} \sim K^*$, below which our perturbative (in γ) RG is no longer trustworthy. Similarly to the case of supercritical disorder in higher dimensions, the momentum $K_{\rm mob}$ corresponds to the mobility threshold $E_{\rm mob}$, if $d > 2$ (in addition to $d < 2\alpha$), all states with $E < E_{\rm mob}$ being localized.

Using the condition $\gamma(K) \sim 1$ and Eqs. (5.16), (5.20), and (6.14), we obtain the mobility threshold in such lower dimensions:

$$E_{\rm mob} = aK_0^\alpha \left(\frac{\varkappa}{a^2 K_0^\varepsilon}\right)^{\frac{1}{4}} \left(1 + \frac{|\varkappa_c|}{\varkappa}\right)^{\frac{1}{4}-\frac{\alpha}{\varepsilon}}. \tag{6.20}$$

Finally, we note, that sufficiently below critical dimension, $\varepsilon \gtrsim 1$, Eq. (5.19) shows that, in agreement with the perturbation theory of Sec. IV, the renormalization of the disorder strength is negligible, i.e., $\tilde{\varkappa}(K) \approx \varkappa$ so long as the disorder is weak, $\gamma \ll 1$. In contrast, just below the critical dimension ($0 < \varepsilon \ll 1$) the parameters of the system are significantly renormalized due to elastic scattering between states in the whole conduction band.

VII. WEYL SEMIMETAL

Weyl semimetal is a 3D material characterized by Dirac quasiparticle dispersion of long-wave excitations,

$$\hat{\mathcal{H}} = v\hat{\boldsymbol{\sigma}} \cdot \mathbf{k}, \tag{7.1}$$

with $\hat{\boldsymbol{\sigma}}$ being a (pseudo)spin-1/2 operator.

Generically, one expects an even number of Dirac points in the first Brillouin zone (a consequence of Dirac fermion doubling problem on a lattice [53]). However, for a sufficiently smooth random potential, that we will assume here for simplicity, scattering between Dirac points (internodal scattering) may be neglected, restricting the analysis to the vicinity of one point only.

We first note that, unlike the case of a semiconductor described by the model (2.1), quasiparticles in Weyl semimetal cannot be localized in the absence of internodal scattering. This follows from the observation that a Weyl fermion is characterized by a nonzero Berry flux through a closed surface surrounding the Dirac point in the momentum space [21]. Thus WSM may be considered as a surface of a 4D topological insulator in the AII class [22]. Surface states of a topological insulator cannot get localized by disorder, and, thus, neither can Weyl fermions near one Dirac point.

Despite the absence of the Anderson transition in Weyl semimetal, a weak-to-strong disorder transition manifests itself in a critical behavior of a variety of physical observables, in particular the disorder-averaged density of states, to whose analysis we now turn.

The RG analysis for disordered materials with Dirac-type quasiparticle dispersion is similar to that for high-dimensional semiconductors, described in Sec. V, and have been carried out in a number of previous works [4–11,13]. The critical dimension in the case of quasiparticles with linear dispersion, Eq. (7.1), is $d_c = 2\alpha = 2$, and thus the RG treatment of disorder and the aforementioned weak-to-strong disorder transition (unlike, conventional semiconductors studied in earlier sections) is of direct physical relevance in 3D Dirac materials, WSM.

In order to have a "controlled" RG calculation in WSM, it is essential to analytically continue the model to an arbitrary dimension d and then perform an $\varepsilon = 2 - d$-expansion. We do this by analytically continuing the quasiparticle dispersion according to

$$\hat{\mathcal{H}} = vk^{\frac{1}{2}+\frac{\varepsilon}{2}}\hat{\boldsymbol{\sigma}} \cdot \mathbf{k}, \tag{7.2}$$

and setting $\varepsilon = -1$ at the end of the calculation.

Perturbative RG analysis, quite similar to that of Sec. V, together with such ε-expansion [5,9,11] leads in the one-loop approximation to the flow equations:

$$\partial_l \lambda = \gamma\lambda/2, \tag{7.3}$$

$$\partial_l \gamma = \varepsilon\gamma + \gamma^2, \tag{7.4}$$

that have the same form as Eqs. (5.13) and (5.14), except for a different prefactor, $1/4 \to 1/2$, in Eq. (7.3) and in the

definition of the dimensionless disorder strength

$$\gamma(K) = \frac{2C_d}{v^2}\tilde{\varkappa}(K)K^{-\varepsilon}. \tag{7.5}$$

Following the scheme of Sec. V, we immediately find the critical exponents in 3D (i.e. for WSM),

$$\nu = 1, \quad z = \tfrac{3}{2}, \tag{7.6}$$

and the critical disorder strength

$$\varkappa_c = \pi^2 v^2 / K_0, \tag{7.7}$$

which have also been obtained in the previous works [5,9,11,13]. The values of the critical exponents close to (7.6) have also been found numerically in Ref. [14].

Although localization in Weyl semimetals is forbidden by symmetry in the absence of internodal scattering, the disorder-driven phase transition manifests itself in the conductivity and the density of states. The conductivity of Weyl semimetals for small finite doping has been calculated microscopically in Ref. [11].

The density of states in a Weyl semimetal can be evaluated similarly to that of a high-dimensional semiconductor, described in detail in Sec. VI, by solving the above flow equations (7.3) and (7.4) and using the quadratic part of the quasiparticle Lagrangian with renormalized couplings, which is justified for weak renormalized disorder $\gamma(K_E) \ll 1$.

In the absence of disorder,

$$\rho^{\text{Weyl}}_{\text{clean}}(E) = \frac{E^2}{2\pi^2 v^3}. \tag{7.8}$$

For disorder strength $\varkappa$ close to the critical $\varkappa_c$, the RG analysis yields

$$\rho(E) \sim \frac{K_0}{v^2}E \tag{7.9}$$

in the energy interval $E^*_{\text{Weyl}} \ll E < vK_0$, where

$$E^*_{\text{Weyl}} = vK_0\left|1 - \frac{\varkappa_c}{\varkappa}\right|^{\frac{3}{2}} \tag{7.10}$$

is the crossover energy scale that for $\varkappa < \varkappa_c$ delineates linear (critical, $E > E^*$) and quadratic (disorder-free, $E < E^*$) behavior of the density of states.

For subcritical disorder, $\varkappa < \varkappa_c$, and energies $0 < E \ll E^*_{\text{Weyl}}$, the flows (7.3) and (7.4) crossover from the vicinity of the critical point to the disorder-free Gaussian fixed point. In this regime, we find the disorder-free E^2 scaling of the density of states as a function of energy, enhanced by a universal singular prefactor that diverges as $\varkappa$ approaches the critical value:

$$\rho(E) = \frac{1}{2\pi^2 v^3}\left(1 - \frac{\varkappa}{\varkappa_c}\right)^{-\frac{3}{2}} E^2. \tag{7.11}$$

A strong random potential, $\varkappa > \varkappa_c$, is relevant, leading to the density of states smeared by disorder and independent of energy in the interval for $|E| \lesssim E^*_{\text{Weyl}}$:

$$\rho(E) \sim \frac{K_0^2}{v}\left(1 - \frac{\varkappa_c}{\varkappa}\right)^{\frac{3}{2}}. \tag{7.12}$$

The critical regimes, described by Eqs. (7.9)–(7.12), are summarized in Fig. 5.

VIII. CONCLUSION

A. Summary

In this work, we have studied noninteracting quasiparticles with power-law dispersion moving in a weak random potential. We demonstrated that in contrast to low dimensions (where for $2 < d < 2\alpha$, a conventional Anderson localization transition takes place), for $d > 2\alpha$, such system in addition exhibits a disorder-driven transition in a new universality class. Among other physical properties, it manifests itself in a universal critical behavior of the disorder-averaged density of states and in the sharp dependence of the mobility threshold on disorder strength $\varkappa$. In particular, the mobility threshold vanishes for $\varkappa$ smaller than a critical value. These results are summarized by Figs. 1–6.

B. Outlook

In light of our finding of a novel localization transition and its phenomenology in high dimensions, natural future research directions include its interplay with interactions, more generic band structures (e.g., including other bands) and disorder symmetries, spin-orbital coupling, magnetic field, etc.

Another issue that our work raises is the nature of the high-dimensional localization transition for $\varkappa < \varkappa_c$, across the mobility edge, located close to the edge of the conduction band. Although one may expect that this transition is in the conventional Anderson-localization class, this question deserves further investigation.

Also, we suggest that a localization transition on the Cayley tree, believed to correspond to the infinite dimension $d = \infty$, deserves further investigation, as it may realize the high-dimensional phenomenology studied here. Indeed, it is well-known that including states with energies far from the Fermi level is necessary to describe localization and transport on Cayley tree [2,54,55], similarly to the case of high-dimensional semiconductors considered in this paper. We thus expect models on Cayley tree to display the striking phenomenology uncovered here, leading to, e.g., a critical behavior of the disorder-averaged density of states or novel universality classes of the localization transition.

Another class of systems that exhibit similar unconventional single-particle interference effects, which involve elastic scattering between all states in the band, is lattice models with strong on-site disorder and weak intersite hopping [56,57], describing, e.g., strongly disordered insulators or granulated superconductors in the insulating states. Because such systems can be analyzed by means of a similar RG approach, with momentum states replaced by (quasi-)localized on-site states, we expect superconductor-insulator transitions and metal-insulator transitions in such systems to display similar phenomenology.

ACKNOWLEDGMENTS

We have benefited from discussions with B. L. Altshuler, V. Dobrosavljević, M. P. A. Fisher, A. Kamenev, B. I. Shklovskii, and C. Tian. Our work has been supported by the Alexander von Humboldt Foundation through the Feodor Lynen Research Fellowship (SVS) and by the NSF grants

DMR-1001240 (L.R. and S.V.S.), DMR-1205303 (V.G. and S.V.S.), PHY-1211914 (V.G. and S.V.S.), and PHY-1125844 (S.V.S.). L.R. also acknowledges The Kavli Institute for Theoretical Physics, where a part of this work was done, for its support through the National Science Foundation under the grant PHY11-25915, as well as a partial support by the Simons Investigator award from the Simons Foundation.

APPENDIX A: MEAN FREE PATH IN A WEAKLY DISORDERED SEMICONDUCTOR

In this Appendix, we compute the mean free path for a quasiparticle with energy E in a d-dimensional semiconductor with short-range-correlated disorder. Let us consider first the case of very weak disorder, $\varkappa \ll \varkappa_c$. Then the mean free path is dominated by elastic scattering in a narrow momentum shell around the surface $ap^\alpha = E$ in momentum space. The renormalizations due to the elastic scattering through the states far from this surface can be neglected.

The self-energy part can then be found by integrating over momentum states $\mathbf{p}$ with energies close to E:

$$\Sigma^R(E) = -\varkappa \int G^R(\mathbf{p},E)\frac{d\mathbf{p}}{(2\pi)^d} \tag{A1}$$

with the bare Green's function

$$G^R(\mathbf{p},E) = (E - ap^\alpha + i0)^{-1}. \tag{A2}$$

The mean free path is then given by

$$\ell(k) = -\frac{v(k)}{2\,\mathrm{Im}\,\Sigma^R(E)}, \tag{A3}$$

where $E = ak^a$ and $v(k) = \alpha a k^{\alpha-1}$ is the velocity corresponding to the momentum k. Using Eqs. (A1)–(A3), we immediately arrive at the result (4.5) for the mean free path in a weakly disordered semiconductor.

If disorder is not very weak ($\varkappa \sim \varkappa_c$ or $\varkappa > \varkappa_c$), quasiparticle properties experience renormalization from elastic scattering between all states in the band. By applying the RG procedure, described in Sec. V, it is possible to remove high momenta from the system and reduce the problem to considering only momentum states with energies close to E.

In particular, if disorder is not very weak but still smaller than critical, $\varkappa < \varkappa_c$, the system flows towards vanishing disorder, and the elastic scattering rate in the renormalized system can be obtained in the Born approximation similarly to the case of a usual low-dimensional metal or a semiconductor [1]. The renormalized disorder strength can be sufficiently small for applying the Born approximation also in the case $\varkappa > \varkappa_c$ and small $\varepsilon = d - 2\alpha \ll 1$, if the RG procedure is terminated by sufficiently large energy E, while the disorder is still weak.

The self-energy part for a quasiparticle with energy E then is given by Eq. (A1) with the replacement $E \to \lambda(k)E$ inside the argument of the Green's function (A2) on the right-hand side,

$$\lambda(k)E = ak^\alpha. \tag{A4}$$

The respective mean free path can be also defined by Eq. (A3), leading to Eq. (4.5). Then the small parameter $\gamma(k) \sim [k\ell(k)]^{-1} \ll 1$ plays the same role in the renormalized system as it does in a usual metal [1] or a very-weakly-disordered nonrenormalized system; it suppresses diagrams with crossed impurity lines.

Indeed, single-particle interference effects involve quasiparticle propagators with equal energies E. The suppression of diagrams with crossed impurity lines occurs due to an additional constraint [1] of the form $|ap_1^\alpha \pm ap_2^\alpha \pm \cdots \pm ap_N^\alpha| \lesssim -\mathrm{Im}\,\Sigma^R(E)$ on the quasiparticle momenta $p_1, p_2, \ldots, p_N$ near the surfaces $ap_1^\alpha = ap_1^\alpha = \cdots = ap_N^\alpha = \lambda(k)E$. Such diagrams are suppressed if $k\ell(k) \gg 1$ with the mean free path $\ell(k)$ defined by Eq. (A3).

APPENDIX B: DETAILS OF THE RG ANALYSIS

In this section, we provide details of the renormalization-group analysis for the density of states (5.6) and the quasiparticle Lagrangian (5.7). On each step of the RG procedure we split the supervectors ψ, $\psi^\dagger$ into the "fast" ψ_f, $\psi_f^\dagger$ and "slow" ψ_s, $\psi_s^\dagger$ parts, including respectively the larger ($Ke^{-l} < k < K$) and the smaller ($k < Ke^{-l}$) momentum components of the fields ψ, $\psi^\dagger$ and, perturbatively in the weak random potential, integrate out the fast components.

The Lagrangian of the quasiparticles separates into a sector containing only fast fields, a sector of the slow fields and the "interaction" Lagrangian $\mathcal{L}_i$ that couples fast and slow degrees of freedom:

$$\mathcal{L}(\psi^\dagger,\psi) = \mathcal{L}(\psi_f^\dagger,\psi_f) + \mathcal{L}(\psi_s^\dagger,\psi_s) + \mathcal{L}_i(\psi_s^\dagger,\psi_s,\psi_f^\dagger,\psi_f), \tag{B1}$$

where $\mathcal{L}(\psi^\dagger,\psi) = \mathcal{L}_0(\psi^\dagger,\psi) + \mathcal{L}_{\mathrm{int}}(\psi^\dagger,\psi)$, Eqs. (5.7) and (5.8), and

$$\begin{aligned}\mathcal{L}_i(\psi_s^\dagger,\psi_s,\psi_f^\dagger,\psi_f) &= \tilde{\varkappa}\int(\psi_f^\dagger\psi_f)(\psi_s^\dagger\psi_s)d\mathbf{r} + \tilde{\varkappa}\int(\psi_s^\dagger\psi_f)(\psi_f^\dagger\psi_s)d\mathbf{r} \\ &+\frac{\tilde{\varkappa}}{2}\int(\psi_f^\dagger\psi_s)(\psi_f^\dagger\psi_s)d\mathbf{r} + \frac{\tilde{\varkappa}}{2}\int(\psi_s^\dagger\psi_f)(\psi_s^\dagger\psi_f)d\mathbf{r}.\end{aligned} \tag{B2}$$

Integrating out the fast field results in (i) the renormalization of the Lagrangian of the slow modes and (ii) the renormalization of the preexponential factor in the expression (5.6) for the density of states.

Renormalized Lagrangian. To the leading order in the small disorder strength (one-loop approximation) the Lagrangian of the slow modes is renormalized according to

$$\mathcal{L}(\psi_s^\dagger,\psi_s) \to \mathcal{L}(\psi_s^\dagger,\psi_s) + \langle\mathcal{L}_i\rangle_f - \tfrac{1}{2} \ll \mathcal{L}_i^2 \gg_f , \tag{B3}$$

where $\langle\ldots\rangle_f = \int \mathcal{D}\psi_f^\dagger\mathcal{D}\psi_f \ldots e^{-\mathcal{L}(\psi_f^\dagger,\psi_f)}$, and $\ll \ldots \gg$ is a similar notation for irreducible (connected) correlators.

The renormalization of the quadratic part of the Lagrangian is determined by the term $\langle\mathcal{L}_i\rangle_f$,

$$\begin{aligned}\delta\mathcal{L}_0(\psi_s^\dagger,\psi_s) = \langle\mathcal{L}_i\rangle_f &= \tilde{\varkappa}\int\langle(\psi_s^\dagger\psi_f)(\psi_f^\dagger\psi_s)\rangle_f d\mathbf{r} \\ &= \int d\mathbf{r}\;\psi_s^\dagger(\mathbf{r})\psi_s(\mathbf{r}) \\ &\cdot\tilde{\varkappa}\int\frac{d\mathbf{p}}{(2\pi)^d}\frac{i}{E\cdot\lambda(K) - ap^\alpha + i0},\end{aligned} \tag{B4}$$

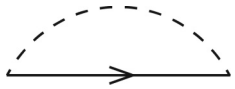

FIG. 9. Diagram corresponding to the renormalization of the quadratic part of the Lagrangian.

and, in terms of the disorder-averaging perturbation theory, corresponds to the diagram in Fig. 9.

In deriving Eq. (B4), we used the correlator

$$\langle \psi_{f\mathbf{k}} \psi^{\dagger}_{f\mathbf{k}} \rangle_f = \mathbb{1}_{FB} \cdot \frac{i}{E \cdot \lambda(K) - ak^{\alpha} + i0} \tag{B5}$$

of the Fourier-transform of the supervectors $\psi^{(\dagger)}_{f\mathbf{k}} = \frac{1}{\sqrt{V}} \int \psi^{(\dagger)}_f(\mathbf{r}) \exp(\mp i\mathbf{kr})\, d\mathbf{r}$, with $\mathbb{1}_{FB}$ being the unity matrix in the space of fermionic and bosonic components of the supervectors.

The renormalization (B4) of the quadratic part of the Lagrangian leads to a shift of the edge of the conduction band and a modification of the coupling λ:

$$\lambda(Ke^{-l}) \cdot E \to \lambda(Ke^{-l}) \cdot E + \lambda(Ke^{-l}) \cdot \delta E + \delta\lambda \cdot E, \tag{B6}$$

where

$$\delta E = \tilde{\varkappa} \int_{Ke^{-l}<p<K} \frac{d\mathbf{p}}{(2\pi)^d} \frac{1}{ap^{\alpha}} = \frac{\tilde{\varkappa} C_d K^{d-\alpha}}{a(d-\alpha)} [1 - e^{-(d-\alpha)l}] \tag{B7}$$

describes the shift of the edge of the band. Throughout the paper, we measure the energy E from the edge of the band, i.e., on each step of the RG procedure absorb δE into the redefinition of the energy E: $E + \delta E \to E$. The modification of the parameter λ in the limit of small $\varepsilon = 2\alpha - d$ reads

$$\delta\lambda = \tilde{\varkappa}\lambda \int_{Ke^{-l}<p<K} \frac{d\mathbf{p}}{(2\pi)^d} \frac{1}{a^2 p^{2\alpha}} \approx \frac{C_d}{a^2} \tilde{\varkappa}\lambda K^{-\varepsilon} \cdot l \tag{B8}$$

and leads to the RG equation (5.9).

The renormalization of the disorder strength $\tilde{\varkappa}$ [of the quartic term in the Lagrangian, Eq. (5.8)] is described by irreducible (connected) pairwise correlators of different terms in the right-hand-side of Eq. (B2) and corresponds to the diagrams in Figs. 8(a)–8(d).

In particular, the contribution of the irreducible (connected) correlator of the first and the second terms in Eq. (B2),

$$\begin{aligned} -\frac{\tilde{\varkappa}^2}{2} \int &\ll [(\psi^{\dagger}_f \psi_f)(\psi^{\dagger}_s \psi_s)](\mathbf{r})[(\psi^{\dagger}_s \psi_f)(\psi^{\dagger}_f \psi_s)](\mathbf{r}') \\ &\gg_f d\mathbf{r} d\mathbf{r}' \\ &= -\frac{\tilde{\varkappa}^2}{2} \int (\psi^{\dagger}_s \psi_s)(\mathbf{r}) \psi^{\dagger}_s(\mathbf{r}') \langle \psi_f(\mathbf{r}') \psi^{\dagger}_f(\mathbf{r}) \rangle_f \\ &\quad \times \langle \psi_f(\mathbf{r}) \psi^{\dagger}_f(\mathbf{r}') \rangle_f \psi_s(\mathbf{r}') d\mathbf{r} d\mathbf{r}', \end{aligned} \tag{B9}$$

equals the diagram in Fig. 8(c). Interchanging the expressions in the square brackets in Eq. (B9) corresponds then to the diagram 8(d), which has the same value. Similarly, the correlator of the second term in Eq. (B2) with itself corresponds to the diagram 8(b), of the third and the fourth terms—to the diagram 8(a). The other correlators vanish. The four correlators, corresponding to the diagrams Fig. 7(a)–7(d), contribute equally to the renormalization of the disorder strength $\varkappa$ and lead to the RG flow equation (5.10).

Preexponential factor renormalization. Integrating out the fast fields ψ_f and $\psi^{\dagger}_f$ renormalizes not only the Lagrangian but also the preexponential factor in the expression for the density of states, Eq. (5.6).

Indeed, due to the correlations between the fast components of the supersymmetry-breaking preexponential factor $\propto \int \psi_{\beta}(\mathbf{r}) \psi^{\dagger}_{\beta}(\mathbf{r}) d\mathbf{r} = \int \psi_{s\beta}(\mathbf{r}) \psi^{\dagger}_{s\beta}(\mathbf{r}) d\mathbf{r} + \int \psi_{f\beta}(\mathbf{r}) \psi^{\dagger}_{f\beta}(\mathbf{r}) d\mathbf{r}$ and the Lagrangian $\mathcal{L}_i$, the former is renormalized as

$$\int \psi^{\dagger}_s(\mathbf{r}) \psi_s(\mathbf{r}) d\mathbf{r} \to \int \psi^{\dagger}_s(\mathbf{r}) \psi_s(\mathbf{r}) d\mathbf{r} - \int \langle \psi_{f\beta}(\mathbf{r}) \psi^{\dagger}_{f\beta}(\mathbf{r}) \mathcal{L}_i(\psi^{\dagger}_s, \psi_s, \psi^{\dagger}_f, \psi_f) \rangle_f d\mathbf{r}. \tag{B10}$$

Using Eqs. (B2), we find straightforwardly that the modification (B10) is equivalent to multiplying $\int \psi^{\dagger}_s(\mathbf{r}) \psi_s(\mathbf{r}) d\mathbf{r}$ by $1 + \delta\lambda/\lambda \equiv \lambda(Ke^{-l})/\lambda(K)$. Therefore, as a result of integrating out the fast fields, the expressions (5.6)–(5.8) reduce to the same form with all the effects of the fast fields encoded in the renormalized parameters λ and $\tilde{\varkappa}$.

[1] A. A. Abrikosov, L. P. Gorkov, and I. E. Dzyaloshinski, *Methods of Quantum Field Theory in Statistical Physics* (Dover, New York, 1975).

[2] K. B. Efetov, *Supersymetry in Disorder and Chaos* (Cambridge University Press, New York, 1999).

[3] A. Kamenev, *Field Theory of Non-Equilibrium Systems* (University Press, Cambridge, 2011).

[4] V. S. Dotsenko and V. S. Dotsenko, Adv. Phys. **32**, 129 (1983).

[5] E. Fradkin, Phys. Rev. B **33**, 3263 (1986).

[6] E. Fradkin, Phys. Rev. B **33**, 3257 (1986).

[7] A. W. W. Ludwig, M. P. A. Fisher, R. Shankar, and G. Grinstein, Phys. Rev. B **50**, 7526 (1994).

[8] A. A. Nersesyan, A. M. Tsvelik, and F. Wenger, Phys. Rev. Lett. **72**, 2628 (1994).

[9] P. Goswami and S. Chakravarty, Phys. Rev. Lett. **107**, 196803 (2011).

[10] I. L. Aleiner and K. B. Efetov, Phys. Rev. Lett. **97**, 236801 (2006).

[11] S. V. Syzranov, L. Radzihovsky, and V. Gurarie, arXiv:1402.3737.

[12] P. M. Ostrovsky, I. V. Gornyi, and A. D. Mirlin, Phys. Rev. B **74**, 235443 (2006).

[13] E.-G. Moon and Y. B. Kim, arXiv:1409.0573.

[14] K. Kobayashi, T. Ohtsuki, K.-I. Imura, and I. F. Herbut, Phys. Rev. Lett. **112**, 016402 (2014).

[15] Z. K. Liu, B. Zhou, Y. Zhang, Z. J. Wang, H. M. Weng, D. Prabhakaran, S.-K. Mo, Z. X. Shen, Z. Fang, X. Dai *et al.*, Science **343**, 864 (2014).
[16] M. Neupane, S.-Y. Xu, R. Sankar, N. Alidoust, G. Bian, C. Liu, I. Belopolski, T.-R. Chang, H.-T. Jeng, H. Lin *et al.*, Nat. Commun. **5**, 3786 (2014).
[17] S. Borisenko, Q. Gibson, D. Evtushinsky, V. Zabolotnyy, B. Büchner, and R. J. Cava, Phys. Rev. Lett. **113**, 027603 (2014).
[18] S. Jeon, B. B. Zhou, A. Gyenis, B. E. Feldman, I. Kimchi, A. C. Potter, Q. D. Gibson, R. J. Cava, A. Vishwanath, and A. Yazdani, Nat. Mater. **13**, 851 (2014).
[19] Z. K. Liu, J. Jiang, B. Zhou, Z. J.Wang, Y. Zhang, H. M.Weng, D. Prabhakaran, S.-K. Mo, H. Peng, P. Dudin *et al.*, Nat. Mat. **13**, 677 (2014).
[20] A. A. Burkov and L. Balents, Phys. Rev. Lett. **107**, 127205 (2011).
[21] X. Wan, A. M. Turner, A. Vishwanath, and S. Y. Savrasov, Phys. Rev. B **83**, 205101 (2011).
[22] S. Ryu, A. Schnyder, A. Furusaki, and A. Ludwig, New J. Phys. **12**, 065010 (2010).
[23] B. Sbierski, G. Pohl, E. J. Bergholtz, and P. W. Brouwer, Phys. Rev. Lett. **113**, 026602 (2014).
[24] Y. Ominato and M. Koshino, Phys. Rev. B **89**, 054202 (2014).
[25] G. Casati, I. Guarneri, and D. L. Shepelyansky, Phys. Rev. Lett. **62**, 345 (1989).
[26] D. R. Grempel, R. E. Prange, and S. Fishman, Phys. Rev. A **29**, 1639 (1984).
[27] F. L. Moore, J. C. Robinson, C. Bharucha, P. E. Williams, and M. G. Raizen, Phys. Rev. Lett. **73**, 2974 (1994).
[28] J. Chabé, G. Lemarié, B. Grémaud, D. Delande, P. Szriftgiser, and J. C. Garreau, Phys. Rev. Lett. **101**, 255702 (2008).
[29] G. Lemarié, J. Chabé, P. Szriftgiser, J. C. Garreau, B. Grémaud, and D. Delande, Phys. Rev. A **80**, 043626 (2009).
[30] P. Markos, Acta Physica Slovaca **56**, 561 (2006).
[31] A. M. Garcia-Garcia and E. Cuevas, Phys. Rev. B **75**, 174203 (2007).
[32] Y. Ueoka and K. Slevin, J. Phys. Soc. Jpn. **83**, 084711 (2014).
[33] I. K. Zharekeshev and B. Kramer, Ann. Phys. (Leipzig) **7**, 442 (1998).
[34] V. F. Gantmakher, *Electrons and Disorder in Solids* (Oxford University Press, New York, 2005).
[35] I. M. Lifshitz, Sov. Phys. JETP **17**, 1159 (1963).
[36] J. Zittartz and J. S. Langer, Phys. Rev. **148**, 741 (1966).
[37] B. I. Halperin and M. Lax, Phys. Rev. **148**, 722 (1966).
[38] I. M. Lifshits, S. A. Gredeskul, and L. A. Pastur, *Introduction to the Theory of Disordered Systems* (Wiley, New York, 1988).
[39] Throughout the paper, by the "bottom of the band" we mean the disorder-renormalized edge of the band, not accounting for the rare-regions effects that lead to the formation of Lifshitz tails (exponentially suppressed in $1/\varepsilon$).
[40] B. I. Shklovskii and A. L.Efros, *Electronic Properties of Doped Semiconductors* (Springer, Heidelberg, 1984).
[41] B. Skinner, Phys. Rev. B **90**, 060202(R) (2014).
[42] V. V. Cheianov, V. I. Falko, B. L. Altshuler, and I. L. Aleiner, Phys. Rev. Lett. **99**, 176801 (2007).
[43] R. Nandkishore, D. A. Huse, and S. L. Sondhi, Phys. Rev. B **89**, 245110 (2014).
[44] A. F. Ioffe, Can. J. Phys. **34**, 1393 (1956).
[45] A. F. Ioffe and A. R. Regel, Prog. Semicond. **4**, 237 (1960).
[46] B. Roy and S. D. Sarma, Phys. Rev. B **90**, 241112(R) (2014).
[47] J. L. Cardy, J. Phys. C: Solid State Phys. **11**, L321 (1978).
[48] S. Yaida, arXiv:1205.0005.
[49] B. Bulka, M. Schreiber, and B. Kramer, Z. Phys. B **66**, 21 (1987).
[50] S. Sachdev, *Quantum Phase Transitions* (Cambridge University Press, New York, 2011).
[51] B. Shapiro and E. Abrahams, Phys. Rev. B **24**, 4889 (1981).
[52] F. Wegner, Z. Phys. B **25**, 327 (1976).
[53] H. B. Nielsen and M. Ninomiya, Nucl. Phys. B **185**, 20 (1981).
[54] R. Abou-Chacra, P. W. Anderson, and D. J. Thouless, J. Phys. C: Solid State Phys. **6**, 1734 (1973).
[55] A. D. Mirlin and Y. V. Fyodorov, Nucl. Phys. B **366**, 507 (1991).
[56] S. V. Syzranov, O. M. Yevtushenko, and K. B. Efetov, Phys. Rev. B **86**, 241102(R) (2012).
[57] S. V. Syzranov, A. Moor, and K. B. Efetov, Phys. Rev. Lett. **108**, 256601 (2012).